

# Critical conditions and breakup of non-squashed microconfined droplets: effects of fluid viscoelasticity

Ruth Cardinaels · Paula Moldenaers

Received: 16 July 2010 / Accepted: 20 October 2010 / Published online: 8 December 2010  
© Springer-Verlag 2010

**Abstract** Droplet breakup in systems with either a viscoelastic matrix or a viscoelastic droplet is studied microscopically in bulk and confined shear flow, using a parallel plate counter rotating shear flow cell. The ratio of droplet diameter to gap spacing is systematically varied between 0.1 and 0.85. In bulk shear flow, the effects of matrix and droplet viscoelasticity on the critical capillary number for breakup are very moderate under the studied conditions. However, in confined conditions a profoundly different behaviour is observed: the critical capillary numbers of a viscoelastic droplet are similar to those of a Newtonian droplet, whereas matrix viscoelasticity causes breakup at a much lower capillary number. The critical capillary numbers are compared with the predictions of a phenomenological model by Minale et al. (Langmuir 26:126–132, 2010); the model results are in qualitative disagreement with the experimental data. It is also found that the critical dimensionless droplet length, the critical capillary number, and the dimensionless droplet length at breakup show a similar dependency on confinement ratio. As a result, confined droplets in a viscoelastic matrix have a smaller dimensionless length at breakup than droplets in a Newtonian matrix, which affects the breakup mode. Whereas confined droplets in a Newtonian matrix can break up into multiple parts, only two daughter droplets are obtained after breakup in a viscoelastic matrix, up to very large confinement ratios.

**Keywords** Droplet breakup · Confinement · Viscoelasticity · Grace curve · Critical capillary number · Critical droplet length

## 1 Introduction

To achieve the diverse and intricate material properties that are demanded nowadays for a wide variety of applications, many complex fluids with an internal microstructure have to be formulated, transported, and processed. In the case of emulsions, the product properties and rheology are largely determined by the mean droplet size and the droplet size distribution. The last decades, the opportunities of microfluidics as a tool for droplet generation and manipulation have elaborately been investigated (Baroud and Willaime 2004; Günther and Jensen 2006; Shui et al. 2007; Teh et al. 2007). In general, microfluidic devices contain a network of small channels that can be connected by means of simple junctions, but also flow-focussing connections or tapered geometries are commonly applied to tailor the droplet characteristics (Christopher and Anna 2007; Teh et al. 2007). Since the droplet size is generally of the order of the dimensions of the channels of the microfluidic device, wall effects can cause deviations from bulk behaviour. This has led to the discovery and development of a wide range of novel applications and many more are expected to follow (Baroud and Willaime 2004; Günther and Jensen 2006; Christopher and Anna 2007; Shui et al. 2007; Teh et al. 2007). One of the assets of microfluidics is its ability to generate arrays of highly uniform droplets, as reviewed by Christopher and Anna (2007).

To gain physical insight in droplet dynamics and droplet breakup, several researchers have studied droplets in a uniform shear field that is generated between moving

R. Cardinaels · P. Moldenaers (✉)  
Department of Chemical Engineering, Katholieke Universiteit  
Leuven, Willem de Croylaan 46, 3001 Leuven, Belgium  
e-mail: paula.moldenaers@cit.kuleuven.be

parallel plates or concentric cylinders. Due to the absence of pressure gradients and the presence of a constant shear rate over the complete channel height, this type of flow facilitates the interpretation of effects of for instance viscoelasticity and geometrical confinement on the droplet dynamics. Apart from being a model flow type, simple shear flow is also the main flow component during polymer processing, mixing and other operations that involve rotating or moving parts. In the absence of buoyancy and inertia, the dynamics of a Newtonian droplet in a Newtonian matrix in bulk shear flow depends on the ratio  $\lambda$  of droplet to matrix viscosity and on the capillary number  $Ca$  ( $=\eta_m \cdot R \cdot \dot{\gamma}/\Gamma$ , with  $\eta_m$  the matrix viscosity,  $R$  the droplet radius,  $\dot{\gamma}$  the shear rate, and  $\Gamma$  the interfacial tension). The droplet deformation increases with increasing capillary number and above a critical value  $Ca_{cr}$ , the droplet deforms irreversibly under flow until it breaks into two or multiple parts. The critical capillary numbers in bulk shear flow have been documented for a broad range of viscosity ratios (Grace 1982). In particular, it has been found that droplets with a viscosity ratio  $\lambda$  above 4 can not be broken in bulk shear flow (Taylor 1934; Rumscheidt and Mason 1961; Grace 1982). At large  $Ca$ , droplets with  $\lambda \geq 4$  rotate away from the direction of maximum stretch towards the flow direction. Hence, an increase of the shear rate merely causes an increase of the rotation rate of the droplet fluid, without enhancing the droplet deformation. The droplet elongation thus remains limited, which prohibits necking and breakup (Taylor 1934).

Droplet dynamics and droplet breakup in confined shear flow have extensively been studied for blends consisting of Newtonian components, as reviewed by Van Puyvelde et al. (2008). For a viscosity ratio of 1, confinement hardly affects the critical capillary number (Sibillo et al. 2006; Vananroye et al. 2006). However, for viscosity ratios below 1, confinement suppresses breakup whereas for viscosity ratios above 1, it promotes breakup. Even droplets with a viscosity ratio larger than 4 can be broken in confined conditions (Vananroye et al. 2006; Janssen and Anderson 2008; Janssen et al. 2010). Janssen et al. (2010) attributed this to a suppression of the rotation of the droplet towards the flow direction, which enhances the droplet elongation and thus promotes breakup. The dependence of  $Ca_{cr}$  on viscosity ratio and geometrical confinement is qualitatively predicted by the phenomenological confined Minale model for ellipsoidal droplets (Minale 2008) and by numerical simulations (Janssen and Anderson 2007; Janssen et al. 2010). It has to be noted that studies on confined single droplets are almost exclusively dealing with droplet sizes smaller than the gap spacing. However, in concentrated blends, several authors obtained droplets and strings with a retracted diameter that is much larger than the gap spacing. These squashed droplets can show

different behavior as compared to the unsquashed ones. Pathak and Migler (2003) for instance observed a stabilization against breakup for a blend with a viscosity ratio of 1. In this study, only non-squashed droplets will be studied.

In general, it has been established that both droplet and matrix viscoelasticity stabilize unconfined droplets against breakup (Elmendorp and Maalcke 1985; Mighri et al. 1998; Lerdwijitjarud et al. 2003; Lerdwijitjarud et al. 2004; Li and Sundararaj 2008). In addition, component viscoelasticity can cause elongation and eventually breakup along the vorticity direction (Migler 2000; Cherdhirankorn et al. 2004; Mighri and Huneault 2006; Tanpaiboonkul et al. 2007; Li and Sundararaj 2008). Contrary to the results for fully Newtonian systems, this mechanism can cause breakup in bulk shear flow at viscosity ratios above 4 (Mighri and Huneault 2006). Data on the dynamics of confined droplets that contain a viscoelastic component are scarce (Cardinaels et al. 2009; Minale et al. 2010; Cardinaels and Moldenaers 2010) and the critical conditions for breakup are unexplored up to now. Recently, it has been suggested that under confined conditions a uniform shear flow can be exploited to generate quasi monodisperse emulsions by controlled breakup at near-critical conditions (Sibillo et al. 2006; Renardy 2007). However, this has only been demonstrated for systems consisting of Newtonian components whereas blend components often have a rather complex flow behaviour, including viscoelasticity and shear thinning. The question then arises whether this technique is also applicable to these blends. In this study, the effect of viscoelasticity of the components on the breakup mode of confined droplets will be investigated systematically. In addition, the conditions that are required to generate near-critical breakup in confinement will be mapped out for blends with either a viscoelastic matrix or a viscoelastic droplet. The results will be used to validate a recently developed phenomenological model for droplet dynamics of confined droplets in systems with viscoelastic components (Minale et al. 2010).

## 2 Materials and methods

Droplet breakup is studied here with a home-built counter rotating shear flow cell, that is an adapted version of a Physica MCR300 rheometer. A schematic of the setup is given in Fig. 1. With this setup, a droplet in the stagnation plane between two parallel plates, that rotate in opposite directions, can be visualized with a non-moving microscope connected to a camera. The relative speed of the plates can be varied while keeping the shear rate in the gap constant. Hence, the position of the stagnation plane can be shifted vertically, thereby providing a means to track the position of the droplet within the gap. Only droplets near

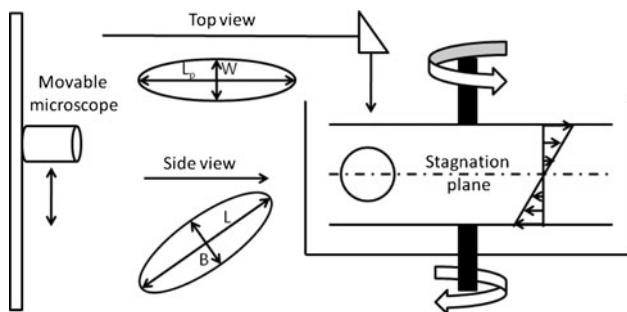


**Fig. 1** Counter rotating shear flow cell and schematic representation of a deformed droplet in the velocity–vorticity (*top view*) and velocity–velocity gradient (*side view*) planes

the midplane of the gap have been used for the breakup experiments. In this study, the droplet dynamics is observed from the top, i.e., in the velocity–vorticity plane. To explore the effects of confinement on droplet breakup, the ratio of droplet diameter  $2R$  to gap spacing  $H$  is varied by adapting the spacing between the plates in the range from 3 to 0.4 mm. The temperature is controlled to within  $0.2^\circ\text{C}$  by controlling the temperature of the room. More details about the experimental setup can be found elsewhere (Vananroye et al. 2006; Verhulst et al. 2007; Cardinaels et al. 2009).

The critical  $Ca$ -numbers for breakup have been determined by increasing  $Ca$  in steps of 0.01. After applying a  $Ca$ -number that does not result in breakup, the droplet was allowed to relax back to the spherical shape before flow with a higher  $Ca$  was started.  $Ca_{cr}$  is defined as the smallest  $Ca$ -number for which droplet breakup was observed. With this direct startup protocol, the ambiguity is avoided of choosing an acceleration or time spend at each  $Ca$ , which can affect  $Ca_{cr}$  obtained from a gradual increase of  $Ca$  (Torza et al. 1972). In addition, literature data for blends containing Newtonian components have also been obtained with this protocol (Vananroye et al. 2006; Janssen et al. 2010). Hence, the data for systems with viscoelastic components can be directly compared to these literature data.

Table 1 gives an overview of the materials and blends that have been used in this study. The properties of the droplet and matrix fluid are denoted with  $d$  and  $m$ . As

viscoelastic material a polyisobutylene (PIB) Boger fluid [BF2 from Verhulst et al. (2007, 2009a)] was prepared. This fluid has a constant viscosity and first normal stress coefficient in the shear rate range of interest. As Newtonian components, PIB and different grades of polydimethylsiloxane (PDMS) have been used. Blends containing either a viscoelastic droplet or a viscoelastic matrix and reference blends consisting of Newtonian components have been prepared with viscosity ratios of 0.45 and 1.5. In addition, a blend with a viscoelastic matrix and a very low viscosity ratio of 0.025 has been used. The interfacial tension of the systems was determined by fitting the slow flow droplet deformation data to the second order theory of Greco (2002). Since PIB is slightly soluble in PDMS (Guido et al. 1999), the PDMS is saturated with low molecular weight PIB when it is used as matrix phase. The thus obtained systems have a constant interfacial tension, that is given in Table 1. It has theoretically been derived that viscoelastic effects show up in the droplet deformation if the ratio of fluid relaxation time to droplet emulsion time becomes on the order of 1 (Greco 2002). This ratio is termed the Deborah number  $De$  ( $=\Psi_1 \cdot \Gamma / (2 \cdot R \cdot \eta^2)$ , with  $\Psi_1$  the first normal stress coefficient and  $\Gamma$  the interfacial tension). In all experiments, the droplet size is controlled (on the order of  $150 \mu\text{m}$ ) to obtain a constant Deborah number of approximately 1. This results in Weissenberg numbers  $Wi$  ( $=\Psi_1 \cdot \dot{\gamma}^2 / \eta \cdot \dot{\gamma}$ ) in bulk conditions between 0.4 and 1.7.

### 3 Experimental results and discussion

#### 3.1 Critical Ca-numbers

##### 3.1.1 Comparison between viscoelastic droplet and viscoelastic matrix

The critical  $Ca$ -numbers ( $Ca_{cr}$ ) for breakup as a function of confinement ratio are given in Fig. 2 for blends with viscoelastic components at viscosity ratios of 1.5 and 0.45. It

**Table 1** Blend and component characteristics

Droplet	Matrix	$T$ ( $^\circ\text{C}$ )	$\eta_m$ ( $\text{Pa s}$ )	$\Psi_{1,d}$ ( $\text{Pa s}^2$ )	$\Psi_{1,m}$ ( $\text{Pa s}^2$ )	$\Gamma$ ( $\text{mN/m}$ )	$\lambda$
PDMS100-200	PIB1300	25.5	83.5	0	0	2.7	1.5
PDMS30-100	BF2	26.4	36.5	0	197	2.0	1.5
BF2	PDMS30	26.0	25.2	212	0	2.2	1.5
PDMS30-60	PIB1300	26.2	74.2	0	0	2.5	0.45
PDMS12,5-30	BF2	26.2	37.2	0	204.5	2.0	0.45
BF2	PDMS100	26.2	82.6	204.5	0	1.85	0.45
PDMS1	BF2	26.0	37.8	0	212	2.0	0.025

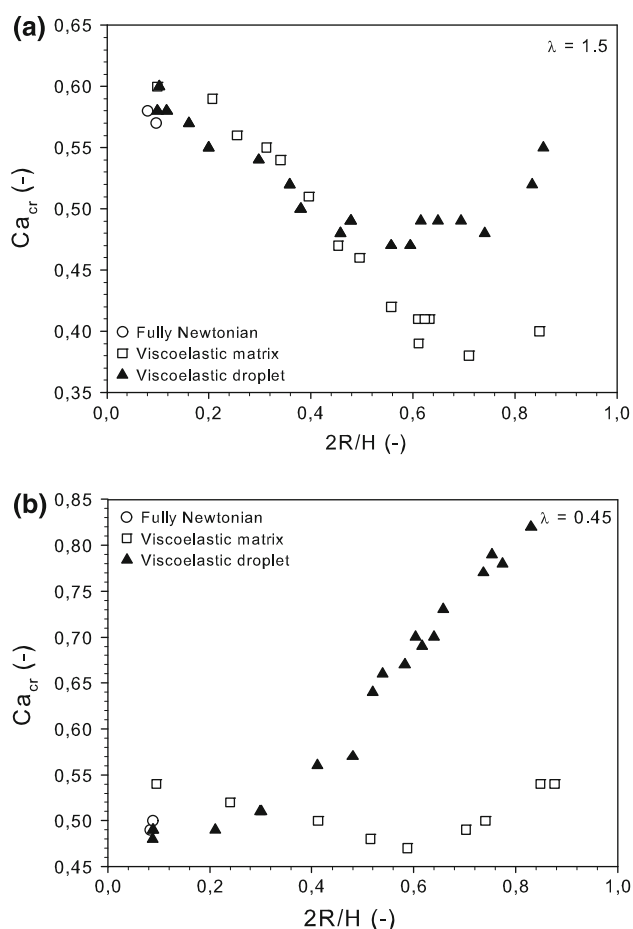


**Fig. 2** Critical Ca-number for breakup as a function of confinement ratio; **a**  $\lambda = 1.5$  and  $De = 1$  and **b**  $\lambda = 0.45$  and  $De = 1$

is clear from Fig. 2 that at low confinement ratios (bulk flow), droplet viscoelasticity with a  $De$ -number of 1 does not influence  $Ca_{cr}$  for both viscosity ratios. Matrix viscoelasticity, however, slightly stabilizes droplets against breakup, an effect that is more pronounced at a viscosity ratio of 0.45 (Fig. 2b) than at  $\lambda = 1.5$  (Fig. 2a). Sibillo et al. (2004) observed an increase of  $Ca_{cr}$  with increasing values of the  $De$ -number of the matrix for systems with different viscosity ratios. The  $De$ -number at which matrix viscoelasticity started to affect  $Ca_{cr}$  was below 1 at a viscosity ratio of 0.6 but above 1 at a viscosity ratio of 2. Hence, the different sensitivity of  $Ca_{cr}$  to matrix viscoelasticity at  $De = 1$  for  $\lambda = 1.5$  and 0.45 is in line with the results of Sibillo et al. (2004). For viscoelastic droplets in a Newtonian matrix, a stabilization against breakup was generally observed (Elmendorp and Maalcke 1985; Migler 2000; Lerdwijitjarud et al. 2003, 2004; Li and Sundararaj 2008). In several studies,  $De$  and  $Wi$  of the droplet were equal to or lower than those used in this study. However, some of the experimental results in the literature may be hampered by effects of shear thinning of the components

and diffusion of the droplet fluid into the matrix phase (Guido et al. 1999). In addition, in all studies except the first one, the critical Ca-number is defined as the highest Ca-number that can be reached without causing the droplet to break during a gradual increase in shear rate. Since viscoelasticity of one of the phases can cause overshoots in the droplet deformation after startup of shear flow, a gradual increase of  $Ca$  can result in profoundly larger critical Ca-numbers as compared to the direct startup experiments that are applied here (Verhulst et al. 2009b).

From Fig. 2 it is clear that confinement substantially affects the critical conditions. It is shown in Fig. 2a that the critical Ca-number for systems with a viscosity ratio of 1.5 initially decreases with increasing degree of confinement. At high confinement ratios,  $Ca_{cr}$  goes through a minimum. If the droplet is viscoelastic, the minimum occurs at a lower confinement ratio as compared to the case when the matrix is viscoelastic. The overall picture is in qualitative agreement with the behaviour of blends with Newtonian components at a viscosity ratio slightly above 1 (Vananroye et al. 2006). A quantitative comparison with the results for blends with Newtonian components will be presented in Sect. 3.1.2

From Fig. 2b it can be concluded that, at a viscosity ratio of 0.45, the variation of  $Ca_{cr}$  as a function of confinement ratio is very moderate for blends with a viscoelastic matrix;  $Ca_{cr}$  only shows a slight minimum at a confinement ratio of about 0.6. The critical Ca-number for viscoelastic droplets is unaffected by confinement up to  $2R/H = 0.4$ . For more confined droplets,  $Ca_{cr}$  increases with increasing confinement ratio, indicating that breakup is suppressed. The latter behaviour is qualitatively similar to that of Newtonian droplets in a Newtonian matrix with a viscosity ratio below 1 (Vananroye et al. 2006; Janssen et al. 2010). In summary, Fig. 2a and b demonstrate that, although the effects of component viscoelasticity on the critical conditions are very moderate in bulk shear flow, droplet and matrix viscoelasticity have a profoundly different effect in confinement. The viscosity ratio is also an important parameter in this respect.

### 3.1.2 Comparison with blends containing Newtonian components for different viscosity ratios

To quantitatively compare the effect of confinement for blends that contain viscoelastic components with blends consisting of Newtonian components, the critical Ca-numbers for the different systems are summarized in Fig. 3. The data are normalized by dividing them with their respective bulk values. Figure 3a displays the experimental results for systems with a viscoelastic droplet and viscosity ratios of 0.45 and 1.5. Results for blends that contain only Newtonian components at viscosity ratios of 0.4 and 1.5

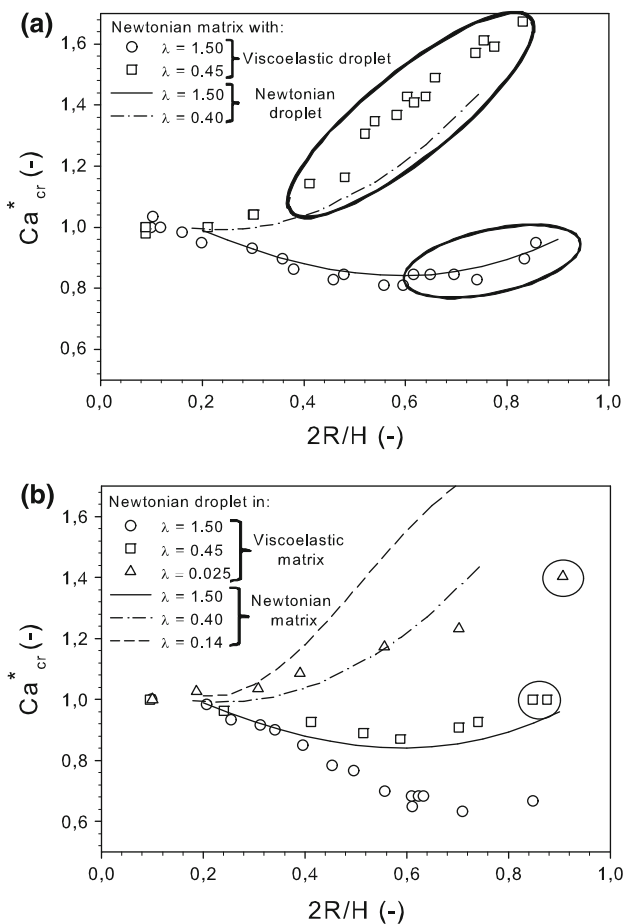


**Fig. 3** Effect of viscosity ratio on the normalized critical Ca-number  $Ca_{cr}^*$  as a function of confinement ratio; **a** Viscoelastic ( $De = 1$ ) or Newtonian droplet in a Newtonian matrix and **b** Newtonian droplet in a Newtonian or a viscoelastic matrix ( $De = 1$ ). Symbols are experimental data for systems with a viscoelastic component and lines are for systems with only Newtonian components [data taken from Janssen et al. (2010) and Vananroye A. (Personal communication 2009)]. Ellipses indicate conditions where multiple neckings occur

are added to this figure. In Fig. 3a it can be seen that, at a viscosity ratio of 1.5 the results for Newtonian and viscoelastic droplets essentially coincide, indicating that droplet viscoelasticity has almost no effect on droplet breakup, neither in bulk nor in confined conditions. The bulk critical capillary numbers for blends with Newtonian components and viscosity ratios of 0.45 and 0.4 are 0.465 and 0.461, respectively (De Bruijn 1989). Due to the minor difference in  $Ca_{cr}$ , results for viscoelastic droplets with  $\lambda = 0.45$  and Newtonian droplets with  $\lambda = 0.4$  can be directly compared. Hence, Fig. 3a shows that droplet viscoelasticity provides a very moderate stabilization against breakup at a viscosity ratio of 0.45.

The normalized critical capillary numbers for systems containing a viscoelastic matrix are compared with their Newtonian counterparts in Fig. 3b. When the matrix is

viscoelastic, an increase of  $Ca_{cr}$  with confinement ratio is barely visible at a viscosity ratio of 0.45 (Fig. 3b) as opposed to a viscoelastic droplet in Fig. 3a. Therefore, additional breakup experiments in a viscoelastic matrix were performed at a very low viscosity ratio of 0.025. It can be seen from Fig. 3b that the normalized critical Ca-number in confined conditions increases when the viscosity ratio is reduced, a trend that is similar to the results for systems with a Newtonian matrix (Fig. 3a and Vananroye et al. (2006)). However, for each viscosity ratio, the normalized critical Ca-numbers for breakup in a viscoelastic matrix are significantly lower than those for Newtonian droplets in a Newtonian matrix. Hence, matrix viscoelasticity promotes breakup of confined droplets under all conditions investigated. It can be noted that for systems with a viscosity ratio of 0.025 no experimental data are available in literature for blends with only Newtonian components but the normalized critical Ca-numbers for droplets in a viscoelastic matrix at  $\lambda = 0.025$  are lower than those for blends with a Newtonian matrix at even higher viscosity ratios. Therefore, the destabilizing effect of matrix viscoelasticity clearly remains present up to very low viscosity ratios.

### 3.1.3 Comparison with predictions of the Minale model

The question now arises if these results can be described by phenomenological models for droplet dynamics, that are available in literature. It is known that the effects of viscosity ratio and geometrical confinement on the critical Ca-numbers in systems with Newtonian components are qualitatively reproduced by the phenomenological Maffettone and Minale (1998) and confined Minale (2008) models. These models describe the dynamics of ellipsoidal droplets in flow by considering a competition between the restoring interfacial forces and the deforming hydrodynamic forces. Recently, these models have been extended to predict droplet dynamics in confined systems with viscoelastic components (Minale et al. 2010). However, this extended model has not yet been validated for droplet breakup. As an example, in Fig. 4 the predicted critical Ca-numbers at a viscosity ratio of 0.45 for systems with viscoelastic components are compared with the experimental data for blends with viscoelastic components and the predictions for the Newtonian reference system at this viscosity ratio. In the calculations,  $Ca_{cr}$  is determined as the smallest value of Ca for which no steady state droplet deformation was obtained. It can be seen from Fig. 4 that there is a large deviation between experimental and model results.

At a viscosity ratio of 1.5, the model predictions show a limiting droplet deformation for large Ca-numbers. Hence, at this viscosity ratio, no critical Ca-number for breakup could be calculated from the model. In summary, it can be



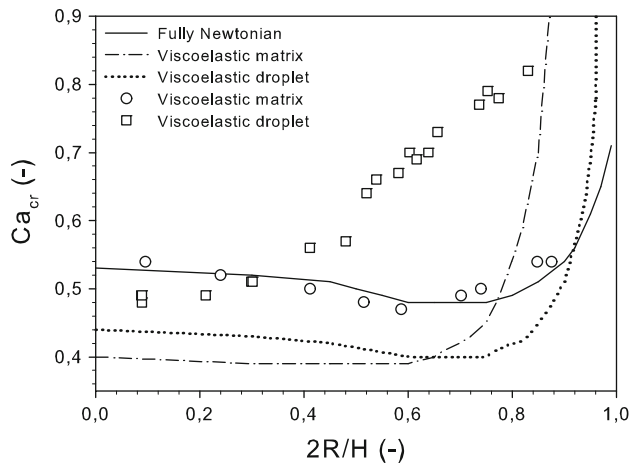


**Fig. 4** Critical Ca-number for breakup as a function of confinement ratio for systems with a viscosity ratio of 0.45; Experimental data (symbols) and predictions of phenomenological models (lines) for systems with Newtonian (Minale 2008) and viscoelastic components ( $De = 1$ ) (Minale et al. 2010)

concluded that the simple phenomenological model for ellipsoidal droplets is not capable of predicting the critical Ca-numbers for blends with viscoelastic components in confined conditions. Most probably, this is caused by the fact that the Minale model has been derived for blends that consist of components that can rheologically be characterized by means of the second-order fluids model. Despite the fact that in the range of shear rates that is relevant in this study, the steady shear rheology of the Boger fluid can be well described by means of this second-order model (Verhulst et al. 2007), Boger fluids have a spectrum of relaxation times and a very high elongational viscosity, two factors that can affect the droplet dynamics. In addition, the Minale model has been developed for ellipsoidal droplets, an assumption that is no longer valid for highly confined droplets at near-critical conditions, as will be discussed in the following sections.

### 3.2 Critical dimensionless droplet length

For systems with Newtonian components in bulk flow, it has been shown that the critical conditions for breakup can be characterized by means of a critical dimensionless droplet length  $L/2R$ ; once the critical value is exceeded the droplet will elongate irreversibly and break up (Grace 1982; Stone et al. 1986). The evolution of this critical value as a function of confinement ratio might contribute to gain insight in the differences between the critical Ca-numbers for confined droplets in systems with either a viscoelastic matrix or a viscoelastic droplet. Experimentally, it has been observed that both component viscoelasticity and geometrical confinement can cause the droplet length after startup of shear flow to go through a

maximum (Sibillo et al. 2006; Vananroye et al. 2008; Verhulst et al. 2009a, 2009b). This maximum at near-critical conditions ( $Ca_{cr} - Ca = 0.01 - 0.02$ ) is used here to characterize the critical dimensionless droplet length. Droplet breakup will occur if the maximum of  $L/2R$  during such a transient exceeds the critical value. This is illustrated in Fig. 5, where the transient droplet length after startup of shear flow is shown for two representative cases. Since the shape of highly deformed droplets deviates from an ellipsoid [see, e.g., Sibillo et al. (2006)], it is not straightforward to define a droplet length and orientation angle unambiguously. The projection of the dimensionless droplet length  $L$  in the velocity direction ( $=L_p/2R$ , Fig. 1) is used in this study to characterize the droplet elongation.

The maximum dimensionless droplet length during startup of shear flow at near-critical conditions is shown in Fig. 6a and b as a function of confinement ratio for viscosity ratios of respectively 1.5 and 0.45. The evolution of the critical dimensionless droplet length in Fig. 6 should be

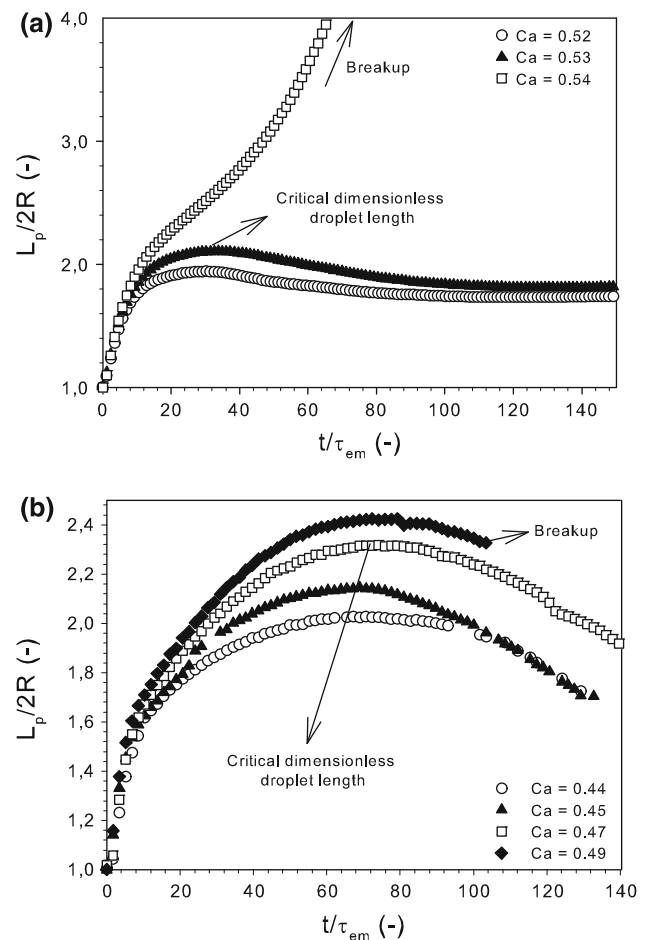


**Fig. 5** Evolution of the dimensionless droplet length after startup of shear flow for various Ca-numbers; **a** Newtonian droplet in a viscoelastic matrix with  $\lambda = 1.5$  and  $2R/H = 0.34$  and **b** Viscoelastic droplet in a Newtonian matrix with  $\lambda = 1.5$  and  $2R/H = 0.62$

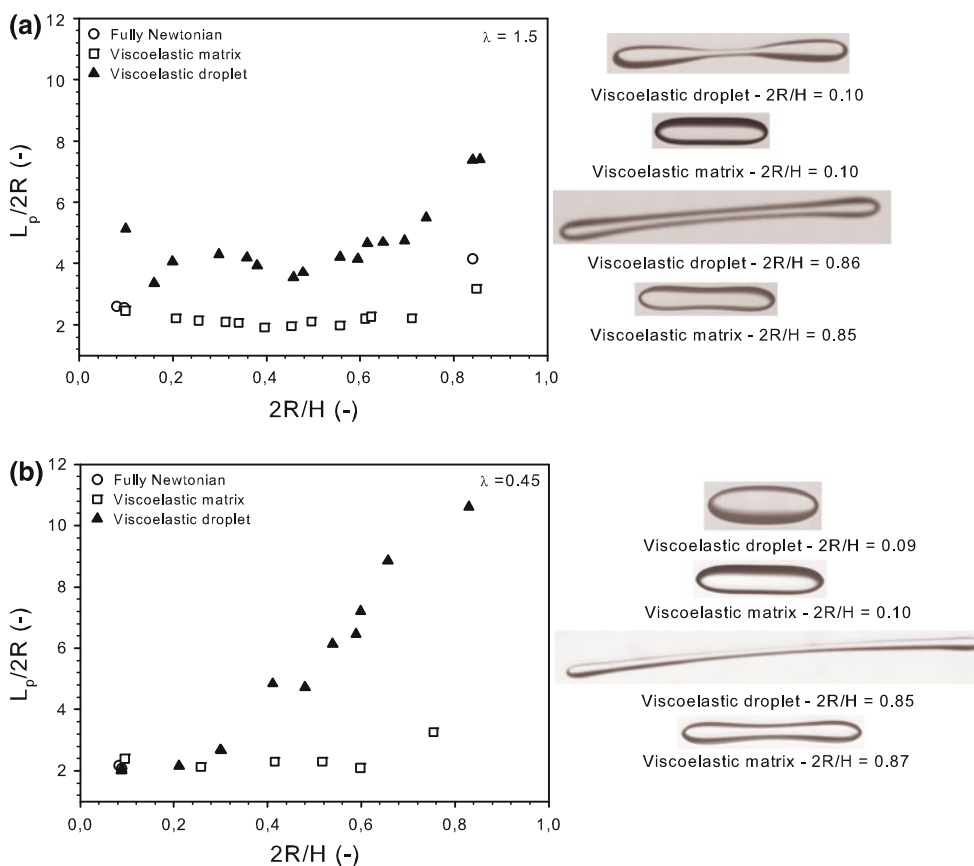


**Fig. 6** Critical dimensionless droplet length  $L_p/2R$  as a function of degree of confinement and corresponding microscopy images in the velocity–vorticity plane for bulk and highly confined conditions; **a**  $\lambda = 1.5$  and **b**  $\lambda = 0.45$

compared with the dependency of  $Ca_{cr}$  on the confinement ratio under the same conditions, as displayed in Fig. 2. When comparing the results at a viscosity ratio of 1.5 (Figs. 2a and 6a) and at a viscosity ratio of 0.45 (Figs. 2b and 6b), it is immediately clear that the trends for the critical capillary number and the critical dimensionless droplet length are quite similar. For both viscosity ratios, the critical dimensionless droplet length starts to increase at approximately the degree of confinement where  $Ca_{cr}$  in Fig. 2 shows an upturn. This clearly shows that the significant differences in the critical capillary numbers of confined droplets in a viscoelastic matrix as compared to confined viscoelastic droplets are caused by the substantial effect of matrix viscoelasticity on the critical dimensionless droplet length of confined droplets.

When inspecting the data in Fig. 6 in more detail, it can be seen that in bulk conditions, the maximum value of  $L_p/2R$  for systems with a viscoelastic droplet or a viscoelastic matrix is equal to that for systems with only Newtonian components at a viscosity ratio of 0.45 (Fig. 6b). The corresponding microscopy images in Fig. 6b show that the most deformed droplet that does not break up in bulk conditions remains rather ellipsoidal. However, at a

viscosity ratio of 1.5 (Fig. 6a), an unbounded viscoelastic droplet can withstand much larger deformations without deforming irreversibly as compared to systems with a Newtonian droplet. The microscopy image for the unconfined viscoelastic droplet in Fig. 6a shows that even droplets with a considerable degree of necking can retract and reach a steady state shape. This is contrary to systems with a viscosity ratio of 0.45 and it is caused by the fact that, for the same viscoelastic droplet fluid, the ratio of the viscoelastic normal stress to the shear stress in the undisturbed flow field is larger for the unconfined system with a viscosity ratio of 1.5 ( $\Psi_1 \cdot \dot{\gamma}^2 / (\eta \cdot \dot{\gamma}) = 1.7$ ), than for the system with a viscosity ratio of 0.45 in bulk conditions ( $(\Psi_1 \cdot \dot{\gamma}^2 / (\eta \cdot \dot{\gamma})) = 0.43$ ). Hence, the viscoelastic stresses generated in the droplet with a viscosity ratio of 1.5 are strong enough to cause retraction of a very elongated droplet, whereas in the system with a viscosity ratio of 0.45, the viscous forces dominate and cause droplet breakup at a much smaller droplet length. Matrix viscoelasticity has no effect in bulk conditions.

In confined conditions, the critical dimensionless droplet length for a viscoelastic droplet substantially increases with increasing values of the degree of confinement (as did  $Ca_{cr}$

in Fig. 2a and b), in particular for the blend with the smallest viscosity ratio of 0.45. For large confinement ratios, the microscopy images in Fig. 6a and b for the confined viscoelastic droplets show that long fibrillar shapes are stable in shear flow, indicating that the presence of the walls generates stabilizing hydrodynamic forces. This is different from the critical dimensionless droplet length for breakup of deformed droplets in quiescent conditions (Cardinaels and Moldenaers 2010), indicating that flow is necessary for the generation of stabilizing forces. When the matrix is viscoelastic, an increase of the critical dimensionless droplet length only occurs at high confinement ratios and it remains rather limited, similar to  $Ca_{cr}$  in Fig. 2a and b. The difference between the critical dimensionless droplet length of a droplet in a viscoelastic matrix and a viscoelastic droplet in a Newtonian matrix gradually increases when the degree of confinement is increased. This is most probably caused by the fact that, in a viscoelastic matrix, confinement increases the viscoelastic stresses around the droplet (Cardinaels et al. 2010), which pull out the droplet ends (Verhulst et al. 2009b). This counteracts the viscous stabilizing effects of the walls, thus causing breakup at much shorter droplet lengths in confined conditions when the matrix is viscoelastic.

It is clear from Fig. 6 that the shape of confined droplets at near-critical conditions significantly deviates from an ellipsoid, which might explain the deviations between the predictions of the confined Minale model and the experimental data in Fig. 4. In summary, it can be concluded from the results in this section that the trends of the critical Ca-number as a function of confinement ratio, as shown in Fig. 2, are governed by the evolution of the critical dimensionless droplet length (Fig. 6) as a function of confinement ratio.

### 3.3 Binary versus multiple droplet breakup

An unbounded droplet that breaks up at the critical Ca-number generally forms two daughter droplets with one or more small satellite droplets in between (Rumscheidt and Mason 1961). Long fibrils, that can be formed in bulk conditions by applying a supercritical Ca-number, break up into a large number of small droplets due to capillary instabilities (Rumscheidt and Mason 1962). However, even at the critical Ca-number, confined droplets can deform into long threads before breakup occurs (Sibillo et al. 2006; Janssen and Anderson 2007, 2008; Janssen et al. 2010). For systems with Newtonian components, this breakup into multiple parts only occurs when  $Ca_{cr}$  increases as a function of confinement ratio and it is promoted by a low viscosity ratio (Janssen et al. 2010). The conditions at which breakup into more than two daughter droplets occurs for systems with one viscoelastic component have not yet been

documented in the literature and have been investigated in this study. These conditions are indicated by the ellipses in Fig. 3. From the results for a viscoelastic droplet in Fig. 3a, it is clear that the transition from binary to ternary breakup coincides with the upturn in  $Ca_{cr}$ , which is similar to the results for systems with only Newtonian components (Janssen et al. 2010). However, the formation of multiple neckings is strongly suppressed in a viscoelastic matrix, even far into the region of increasing critical Ca-numbers, as can be seen in Fig. 3b.

In order to quantitatively study the effects of component viscoelasticity and geometrical confinement on the breakup process, the dimensionless droplet length at breakup was determined for the conditions shown in Fig. 2. This dimensionless droplet length at breakup was defined as the dimensionless length of the droplet at the moment just before breakup occurs. Similar to the results in Sect. 3.2, the projection of the droplet length in the velocity direction ( $=L_p$  in Fig. 1) is used to characterize the droplet length at breakup. The results are shown in Fig. 7a and b for viscosity ratios of 1.5 and 0.45, respectively. From a comparison between Fig. 2a and b on one hand and Fig. 7a and b on the other hand, it is clear that the trends in  $Ca_{cr}$  as a function of confinement ratio are reflected in the curves of the dimensionless droplet length at breakup. The dimensionless droplet length at breakup is thus directly related to the Ca-number that causes breakup. For bulk conditions, Sibillo et al. (2004) demonstrated that the pinch-off length shows the same trend as a function of the De-number of the matrix phase as the critical Ca-number. Similar to the results in Sect. 3.2, it is shown here that the relation between critical Ca-number and pinch-off length remains valid in confined conditions. This relation is caused by the fact that an increase of the Ca-number at breakup speeds up the elongation of the droplet, which allows the formation of a longer and thinner thread before instabilities cause necking. An increase of the dimensionless breakup time as a function of confinement ratio, as reported by Sibillo et al. (2006) was not observed in this study, neither for systems with a viscoelastic matrix nor for systems with a viscoelastic droplet.

The evolution of the dimensionless droplet length at breakup with increasing degree of confinement (Fig. 7) can also be compared to that of the critical dimensionless droplet length (Fig. 6). Since it was shown that both parameters are linked to the critical Ca-number, they vary in a similar way with confinement ratio. However, when a quantitative comparison is made, some differences can be observed. In bulk conditions, the dimensionless droplet length at breakup is substantially larger than the critical dimensionless droplet length. This is caused by the fact that the droplet continues to elongate once the critical dimensionless droplet length is exceeded whereas necking only



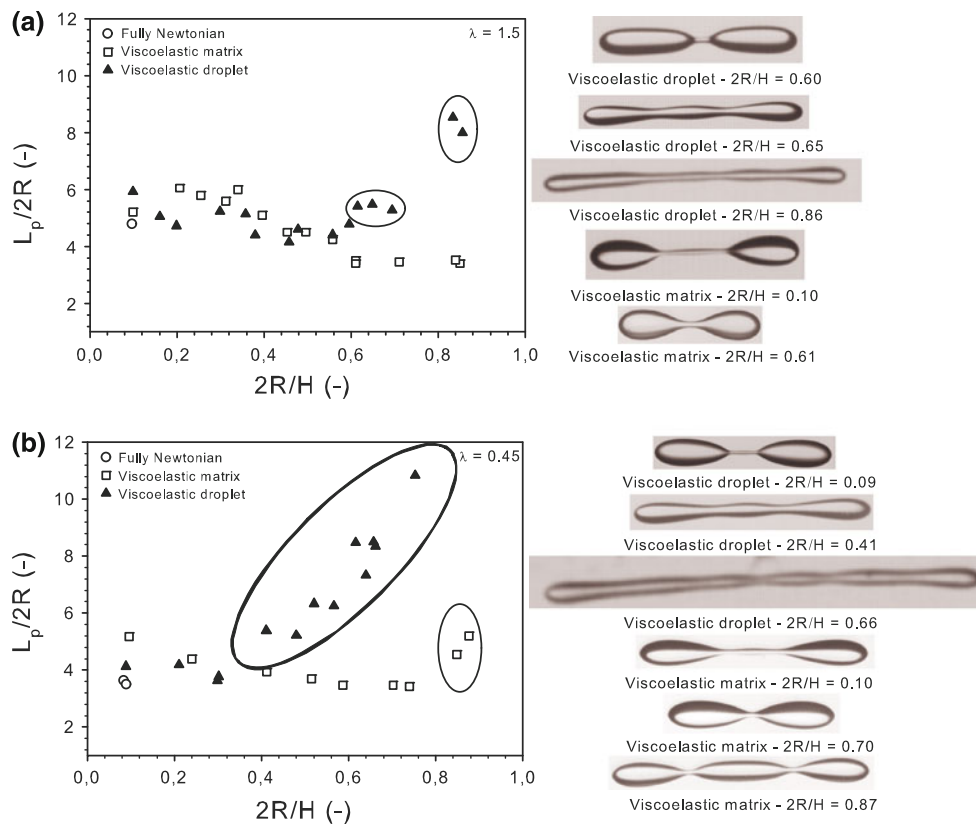


**Fig. 7** Dimensionless projection  $L_p$  of the droplet length at breakup as a function of confinement ratio (ellipses indicate conditions where multiple neckings occur) and microscopy images in the velocity–vorticity plane for selected degrees of confinement; **a**  $\lambda = 1.5$ , **b**  $\lambda = 0.45$

occurs after further thinning. This breakup process is illustrated in Fig. 5a. The exception to this common bulk breakup process is the viscoelastic droplet at  $\lambda = 1.5$  for which droplets with a considerable degree of necking can still retract, as shown in Fig. 6. When the neck has become too thin during droplet elongation, breakup occurs during retraction of the droplet, as illustrated in Fig. 5b. Hence, the critical dimensionless droplet length and the dimensionless droplet length at breakup have a similar value. For all systems, the dimensionless droplet length at breakup and the critical dimensionless droplet length become more or less equal for confined droplets. Under these conditions, breakup proceeds as in Fig. 5b: during retraction of the droplet or fibril, it develops neckings and breaks.

It is clear from Fig. 7 that viscoelastic droplets can become highly elongated before they break in confined conditions. These highly elongated droplets form multiple neckings due to capillary instabilities, as depicted in the microscopy images in Fig. 7; the number of neckings increases with increasing values of the dimensionless droplet length at breakup. However, more than two neckings do not necessarily cause the formation of four or more droplets. Clearly, some neckings grow faster, leading to breakup into less daughter droplets or droplets of different sizes. Therefore, a whole range of numbers and sizes

of droplets can be generated in a confined shear flow, depending on the conditions. This is similar to the observations that were made by Sibillo et al. (2006) for blends with Newtonian components. Studying these effects in detail is however beyond the scope of this study.

As early as 1878, it was already known that instabilities at the interface of a long thread will only grow if the wavelength of the instability exceeds the circumference of the cross section of the thread (Rayleigh 1878). Therefore, only if the thread becomes sufficiently long, multiple neckings can occur at regular distances along the droplet axis. For Newtonian reference systems, it can roughly be estimated that, in order to enable breakup into multiple droplets, the droplet length should be at least six times the undeformed droplet radius (Janssen et al. 2010). The fact that matrix viscoelasticity causes breakup at a much smaller dimensionless droplet length, suppresses the formation of multiple daughter droplets in these systems. Therefore, when the matrix is viscoelastic, breakup into multiple parts only occurs at very high confinement ratios, as shown in Fig. 7b. In addition, for these systems, a reduction of the dimensionless droplet length at breakup with increasing confinement ratio occurs in the region where  $Ca_{cr}$  shows the same trend. From the microscopy images in Fig. 7 it can be seen that this reduction of the

dimensionless droplet length at breakup is mainly caused by the fact that the length of the filament between the two end bulbs of the droplet decreases with increasing degree of confinement. This is similar to breakup under supercritical conditions, for which it was shown that at higher Ca-numbers, the droplet elongates more before breakup occurs (Grace 1982). The reduction of the length of the filament between the daughter droplets causes breakup in confined conditions without generating satellite droplets, which enables the formation of emulsions with a uniform droplet size. In blends with a Newtonian matrix on the other hand, this is only possible over a limited range of degrees of confinement, whereas more confined droplets break up into multiple, but not necessarily equal parts.

Finally, it can be noted that no vorticity elongation, which was often encountered in systems with viscoelastic components (Levitt et al. 1996; Migler 2000; Mighri and Huneault 2001; Cherdhirankorn et al. 2004; Mighri and Huneault 2006; Tanpaiboonkul et al. 2007; Li and Sundararaj 2008), has been observed in this study, neither in bulk, nor in confined conditions. Vorticity elongation has been attributed to normal stresses, either in the droplet or in the matrix fluid (Levitt et al. 1996; Migler 2000). The common aspect in all studies in which vorticity elongation has been observed is the fact that the critical Ca-numbers are an order of magnitude larger than  $Ca_{cr}$  for Newtonian droplets in a Newtonian matrix. Causes for these larger values of  $Ca_{cr}$  are viscosity ratios above 4, two viscoelastic phases that are entangled polymer melts or the use of a gradual stepup in shear rate. Hence, the large shear rates that correspond to these large Ca-numbers cause substantial normal stresses in the viscoelastic fluids, thereby inducing vorticity elongation. Most probably, the absence of vorticity elongation in this study is due to the limited values of Ca and Wi.

#### 4 Conclusions

The combined effects of component viscoelasticity and geometrical confinement on droplet breakup in shear flow have been studied experimentally. The blends under investigation contain either a viscoelastic Boger fluid droplet or a viscoelastic Boger fluid matrix. For a viscoelastic droplet in a Newtonian matrix, the critical conditions for breakup show the same trends as for Newtonian droplets: for viscosity ratios below 1, confinement increases the critical capillary number, for viscosity ratios above 1, the critical Ca-number is reduced over a wide range of confinement ratios. However, when the matrix is viscoelastic, the critical Ca-numbers in confinement are much smaller as compared to the values for systems with a Newtonian matrix. In addition, a much lower viscosity

ratio is needed before confinement can suppress breakup. The phenomenological Minale model (Minale et al. 2010) is not capable of describing the observations. As a full rheological characterization of the used Boger fluid, both in shear and elongational flow, can be found in literature (Verhulst et al. 2007, 2009a), the presented experimental data set can be used for the future development of numerical codes or models.

The evolution of the critical Ca-number with degree of confinement is clearly very similar to the evolution of the maximal droplet elongation that does not cause breakup. In addition, the dependency of the dimensionless droplet length at breakup on the confinement ratio is governed by the evolution of the critical Ca-number at breakup as a function of confinement ratio. These observations extend literature results in bulk conditions to confined conditions. It can thus be concluded that the relation between the maximal dimensionless droplet length that does not cause breakup (critical dimensionless droplet length) as well as the dimensionless droplet length at breakup on one hand and the critical Ca-number on the other hand is universal.

In confinement, the presence of the walls enables the formation of very elongated droplets, mainly at high confinement ratios and for systems with a low viscosity ratio. These highly elongated droplets can break up into multiple parts. Matrix viscoelasticity suppresses the generation of highly elongated droplets and therefore breakup in a viscoelastic matrix generally results in two equal-sized daughter droplets, up to rather large confinement ratios. For all systems, confinement prevents the generation of satellite droplets in between the main daughter droplets, which aids in the formation of emulsions with a uniform droplet size. In general, it can be concluded that the effects of matrix viscoelasticity on the droplet deformation under near-critical conditions and on the critical Ca-number are much more pronounced in highly confined conditions as compared to bulk conditions. Therefore, component viscoelasticity is a factor that should not be neglected in the design of microfluidic devices and micro-scale polymer processing equipment for multiphase systems.

**Acknowledgments** R. Cardinaels is indebted to the Research Foundation-Flanders (FWO) for a Ph. D. Fellowship. This study is supported by Onderzoeksfonds K.U. Leuven (GOA09/002). A. Vananroye is acknowledged for providing the Newtonian reference data in Fig. 3.

#### References

- Baroud CN, Willaime H (2004) Multiphase flows in microfluidics. *C R Physique* 5:547–555
- Cardinaels R, Moldenaers P (2010) Relaxation of fibrils in blends with one viscoelastic component: bulk and confined conditions. *J Polym Sci B Polym Phys* 48:1372–1379

- Cardinaels R, Verhulst K, Moldenaers P (2009) Influence of confinement on the steady state behaviour of single droplets in shear flow for blends with one viscoelastic component. *J Rheol* 53:1403–1424
- Cardinaels R, Afkhami S, Renardy Y, Moldenaers P (2010) An experimental and numerical investigation of the dynamics of microconfined droplets in systems with one viscoelastic phase. *J Non-Newton Fluid Mech*. doi:10.1016/j.jnnfm.2010.10.005
- Cherdhirankorn T, Lerdwijitjarud W, Sirivat A, Larson RG (2004) Dynamics of vorticity stretching and breakup of isolated viscoelastic droplets in an immiscible viscoelastic matrix. *Rheol Acta* 43:246–256
- Christopher GF, Anna SL (2007) Microfluidic methods for generating continuous droplet streams. *J Phys D Appl Phys* 40:R319–R336
- De Bruijn RA (1989) PhD Thesis, Eindhoven University of Technology, The Netherlands
- Elmendorp JJ, Maalcke RJ (1985) A study on polymer blending microrheology: part 1. *Polym Eng Sci* 25:1041–1047
- Grace HP (1982) Dispersion phenomena in high viscosity immiscible fluid systems and application of static mixers as dispersion devices in such systems. *Chem Eng Commun* 14:225–277
- Greco F (2002) Drop deformation for non-Newtonian fluids in slow flows. *J Non-Newton Fluid Mech* 107:111–131
- Günther A, Jensen KF (2006) Multiphase microfluidics: from flow characteristics to chemical and materials synthesis. *Lab Chip* 6:1487–1503
- Guido S, Simeone M, Villone M (1999) Diffusion effects on the interfacial tension of immiscible polymer blends. *Rheol Acta* 38:287–296
- Janssen PJA, Anderson PD (2007) Boundary-integral method for drop deformation between parallel plates. *Phys Fluids* 19:043602/1–013602/11
- Janssen PJA, Anderson PD (2008) A boundary-integral model for drop deformation between two parallel plates with non-unit viscosity ratio drops. *J Comp Phys* 227:8807–8819
- Janssen PJA, Vananroye A, Van Puyvelde P, Moldenaers P, Anderson PD (2010) Generalized behavior of the breakup of viscous drops in confinements. *J Rheol* 54:1047–1060
- Lerdwijitjarud W, Larson RG, Sirivat A, Solomon MJ (2003) Influence of weak elasticity of dispersed phase on droplet behavior in sheared polybutadiene/poly(dimethyl siloxane) blends. *J Rheol* 47:37–58
- Lerdwijitjarud W, Sirivat A, Larson RG (2004) Influence of dispersed-phase elasticity on steady-state deformation and breakup of droplets in simple shearing flow of immiscible polymer blends. *J Rheol* 48:843–862
- Levitt L, Macosko CW, Pearson SD (1996) Influence of normal stress difference on polymer drop deformation. *Polym Eng Sci* 36:1647–1655
- Li H, Sundararaj U (2008) Does drop size affect the mechanism of viscoelastic drop breakup? *Phys Fluids* 20:053101/1–053101/6
- Maffettone PL, Minale M (1998) Equation of Change for ellipsoidal drops in viscous flow. *J Non-Newton Fluid Mech* 78:227–241
- Mighri F, Huneault MA (2001) Dispersion visualization of model fluids in a transparent Couette flow cell. *J Rheol* 45:783–797
- Mighri F, Huneault MA (2006) In situ visualization of drop deformation, erosion, and breakup in high viscosity ratio polymeric systems under high shearing stress conditions. *J Appl Polym Sci* 100:2582–2591
- Mighri F, Carreau PJ, Aji A (1998) Influence of elastic properties on drop deformation and breakup in shear flow. *J Rheol* 42:1477–1490
- Migler KB (2000) Droplet vorticity alignment in model polymer blends. *J Rheol* 44:277–290
- Minale M (2008) A phenomenological model for wall effects on the deformation of an ellipsoidal drop in viscous flow. *Rheol Acta* 47:667–675
- Minale M, Caserta S, Guido S (2010) Microconfined shear deformation of a droplet in an equiviscous non-newtonian immiscible fluid: experiments and modelling. *Langmuir* 26:126–132
- Pathak JA, Migler KB (2003) Droplet-string deformation and stability during microconfined shear flow. *Langmuir* 19:8667–8674
- Rayleigh L (1878) On the instability of jets. *Proc Lond Math Soc* 10:4–13
- Renardy Y (2007) The effects of confinement and inertia on the production of droplets. *Rheol Acta* 46:521–529
- Rumscheidt FD, Mason SG (1961) Particle motions in sheared suspensions XII. Deformation and burst of fluid drops in shear and hyperbolic flow. *J Colloid Sci* 16:238–261
- Rumscheidt FD, Mason SG (1962) Break-up of stationary liquid threads. *J Colloid Sci* 17:260–269
- Shui L, Eijkel JCT, van den Berg A (2007) Multiphase flow in microfluidic systems—control and applications of droplets and interfaces. *Adv Colloid Int Sci* 133:35–49
- Sibillo V, Simeone M, Guido S (2004) Break-up of a Newtonian drop in a viscoelastic matrix under simple shear flow. *Rheol Acta* 43:449–456
- Sibillo V, Pasquariello G, Simeone M, Cristini V, Guido S (2006) Drop deformation in microconfined shear flow. *Phys Rev Lett* 97:054502/1–054502/4
- Stone HA, Bentley BJ, Leal LG (1986) An experimental study of transient effects in the breakup of viscous drops. *J Fluid Mech* 173:131–158
- Tanpaiboonkul P, Lerdwijitjarud W, Sirivat A, Larson RG (2007) Transient and steady-state deformations and breakup of dispersed-phase droplets of immiscible polymer blends in steady shear flow. *Polymer* 48:3822–3835
- Taylor GI (1934) The formation of emulsions in definable fields of flow. *Proc Roy Soc Lond A* 146:501–523
- Teh S-Y, Lin R, Hung L-H, Lee AP (2007) Droplet microfluidics. *Lab Chip* 8:198–220
- Torza S, Cox RG, Mason SG (1972) Particle motions in sheared suspensions XXVII Transient and steady deformation and burst of liquid drops. *J Colloid Int Sci* 38:395–411
- Vananroye A, Van Puyvelde P, Moldenaers P (2006) Effect of confinement on droplet breakup in sheared emulsions. *Langmuir* 22:3972–3974
- Vananroye A, Cardinaels R, Van Puyvelde P, Moldenaers P (2008) Effect of confinement and viscosity ratio on the dynamics of single droplets during transient shear flow. *J Rheol* 52:1459–1475
- Van Puyvelde P, Vananroye A, Cardinaels R, Moldenaers P (2008) Review on morphology development of immiscible blends in confined shear flow. *Polymer* 49:5363–5372
- Verhulst K, Moldenaers P, Minale M (2007) Drop shape dynamics of a Newtonian drop in a non-Newtonian matrix during transient and steady shear flow. *J Rheol* 51:261–273
- Verhulst K, Cardinaels R, Moldenaers P, Renardy Y, Afkhami S (2009a) Influence of viscoelasticity on drop deformation and orientation in shear flow Part 1. Stationary states. *J Non-Newton Fluid Mech* 156:29–43
- Verhulst K, Cardinaels R, Moldenaers P, Afkhami S, Renardy Y (2009b) Influence of viscoelasticity on drop deformation and orientation in shear flow. Part 2: Dynamics. *J Non-Newton Fluid Mech* 156:44–57